Chirality in nonlinear-optical response of planar *G*-shaped nanostructures

E.A. Mamonov,[1] T.V. Murzina,[1,*] I.A. Kolmychek,[1] A.I. Maydykovsky,[1] V.K. Valev,[2] A.V. Silhanek,[3,4] T. Verbiest,[2] V.V. Moshchalkov,[3] and O.A. Aktsipetrov[1]

[1] *Department of Physics, M.V. Lomonosov Moscow State University, Leninskie Gory, Moscow 119991, Russia*

[2] *Molecular Electronics and Photonics, INPAC, Katholieke Universiteit Leuven, Celestijnenlaan 200 D, B-3001 Leuven, Belgium*

[3] *Nanoscale Superconductivity and Magnetism & Pulsed Fields Group, INPAC, Katholieke Universiteit Leuven, Celestijnenlaan 200 D, B-3001 Leuven, Belgium*

[4] *Département de Physique, Université de Liège, B- 4000 Liège, Belgium*

[*] *murzina@shg.ru*

Abstract: Chirality effects in optical second harmonic generation (SHG) are studied in periodic planar arrays of gold *G*-shaped nanostructures. We show that *G*-shaped structures of different handedness demonstrate different SHG efficiency for the *left* and *right* circular polarizations, as well as the opposite directions of the SHG polarization plane rotation. The observed effects are interpreted as the appearance of chirality in the SHG response which allows clear distinguishing of two enantiomers.

OCIS codes: (160.3918) Metamaterials; (160.1585) Chiral media; (190.2620) Harmonic generation and mixing

References and links

1. A. Papakostas, A. Potts, D. M. Bagnall, S. L. Prosvirnin, H. J. Coles, and N. I. Zheludev, "Optical manifestations of planar chirality," Phys. Rev. Lett. **90**, 107404 (2003).
2. S. V. Zhukovsky, A. V. Novitsky, and V. M. Galynsky, "Elliptical dichroism: operating principle of planar chiral metamaterials," Opt. Lett. **34**, 1988–1990 (2009).
3. V. A. Fedotov, A. S. Schwanecke, N. I. Zheludev, V. V. Khardikov, and S. L. Prosvirnin, "Asymmetric transmission of light and enantiomerically sensitive plasmon resonance in planar chiral nanostructures," Nano. Lett. **7**, 1996–1999 (2007).
4. A. Potts, A. Papakostas, D. M. Bagnall, and N. I. Zheludev, "Planar chiral meta-materials for optical applications," Microelectron. Eng. **73-74**, 367–371 (2004).
5. V. K. Valev, A. V. Silhanek, N. Smisdom, B. D. Clercq, W. Gillijns, O. A. Aktsipetrov, M. Ameloot, V. V. Moshchalkov, and T. Verbiest, "Linearly polarized second harmonic generation microscopy reveals chirality," Opt. Express **18**, 8286–8293 (2010).
6. S. Zhang, Y.-S. Park, J. Li, X. Lu, W. Zhang, and X. Zhang, "Negative refractive index in chiral metamaterials," Phys. Rev. Lett. **102**, 023901 (2009).
7. D.-H. Kwon, P. L. Werner, and D. H. Werner, "Optical planar chiral metamaterial designs for strong circular dichroism and polarization rotation," Opt. Express **16**, 11802–11807 (2008).
8. V. A. Fedotov, P. L. Mladyonov, S. L. Prosvirnin, A. V. Rogacheva, Y. Chen, and N. I. Zheludev, "Asymmetric propagation of electromagnetic waves through a planar chiral structure," Phys. Rev. Lett. **97**, 167401 (2006).
9. O. A. Aktsipetrov, T. V. Murzina, E. M. Kim, R. V. Kapra, A. A. Fedyanin, M. Inoue, A. F. Kravets, S. V. Kuznetsova, M. V. Ivanchenko, and V. G. Lifshits, "Magnetization-induced second- and third-harmonic generation in magnetic thin films and nanoparticles," J. Opt. Soc. Am. B **22**, 138–147 (2005).
10. C. Hubert, L. Billot, P.-M. Adam, R. Bachelot, P. Royer, J. Grand, D. Gindre, K. D. Dorkenoo, and A. Fort, "Role of surface plasmon in second harmonic generation from gold nanorods," Appl. Phys. **90**, 181105 (2007).

#159711 - $15.00 USD Received 9 Dec 2011; revised 4 Jan 2012; accepted 5 Jan 2012; published 28 Mar 2012

11. Y. Pu, R. Grange, C.-L. Hsieh, and D. Psaltis, "Nonlinear optical properties of core-shell nanocavities for enhanced second-harmonic generation," Phys. Rev. Lett. **104**, 207402 (2010).
12. J. Butet, J. Duboisset, G. Bachelier, I. Russier-Antoine, E. Benichou, C. Jonin, and P.-F. Brevet, "Optical second harmonic generation of single metallic nanoparticles embedded in a homogeneous medium," Nano. Lett. **10**, 1717–1721 (2010).
13. A. Belardini, M. C. Larciprete, M. Centini, E. Fazio, C. Sibilia, M. Bertolotti, A. Toma, D. Chiappe, and F. B. de Mongeot, "Tailored second harmonic generation from self-organized metal nano-wires arrays," Opt. Express **17**, 3603–3609 (2009).
14. Y. Zeng and J. V. Moloney, "Volume electric dipole origin of second-harmonic generation from metallic membrane with noncentrosymmetric patterns," Opt. Lett. **34**, 2844–2846 (2009).
15. S. Kujala, B. K. Canfield, M. Kauranen, Y. Svirko, and J. Turunen, "Multipole interference in the second-harmonic optical radiation from gold nanoparticles," Phys. Rev. Lett. **98**, 167403 (2007).
16. J. Butet, G. Bachelier, I. Russier-Antoine, C. Jonin, E. Benichou, and P.-F. Brevet, "Interference between selected dipoles and octupoles in the optical second-harmonic generation from spherical gold nanoparticles," Phys. Rev. Lett. **105**, 077401 (2010).
17. Y. Zeng, W. Hoyer, J. Liu, S. W. Koch, and J. V. Moloney, "Classical theory for second-harmonic generation from metallic nanoparticles," Phys. Rev. B **79**, 235109 (2009).
18. W. L. Schaich, "Second harmonic generation by periodically-structured metal surfaces," Phys. Rev. B **78**, 195416 (2008).
19. V. K. Valev, A. V. Silhanek, N. Verellen, W. Gillijns, P. Van Dorpe, O. A. Aktsipetrov, G. A. E. Vandenbosch, V. V. Moshchalkov, and T. Verbiest, "Asymmetric optical second-harmonic generation from chiral *G*-shaped gold nanostructures," Phys. Rev. Lett. **104**, 127401 (2010).
20. S.-M. F. Nee, "Polarization measurement," in *The Measurement, Instrumentation and Sensors Handbook*, J. G. Webster, ed. (CRC and IEEE, Boca Raton, 1999).
21. E. A. Mamonov, T. V. Murzina, I. A. Kolmychek, A. I. Maydykovsky, V. K. Valev, A. V. Silhanek, E. Ponizovskaya, A. Bratkovsky, T. Verbiest, V. V. Moshchalkov, and O. A. Aktsipetrov, "Coherent and incoherent second harmonic generation in planar *G*-shaped nanostructures," Opt. Lett. **36**, 3681–3683 (2011).

1. Introduction

Interaction of electromagnetic waves with artificial nanostructures is of high interest nowadays. A special place here belongs to chiral objects, which possess optical activity and thus allow to control over the polarization state of light. The rotation of the polarization plane of a beam transmitted through an optically active 3D medium can arise due to different values of the refractive and absorption coefficients for the *left* and *right* circularly polarized light, which leads to the opposite directions of the polarization rotation for *left*- and *right*-handed 3D media. The concept of chirality in case of planar objects is the same as for 3D ones and involves the lack of a mirror symmetry in the plane of the structure [1]. In case of 2D objects the bulky helical structure does not exist, while the chirality may originate from the shape of a single elementary part [1–4] as well as from an asymmetrical arrangement of the elements [5–8]. Planar chiral nanostructures can be used for the composition of negative refractive metamaterials, as chirality can suppress the refractive index of light of a certain handedness. In full analogy with 3D chiral media, chiral properties of 2D structures can be revealed when studying the polarization state of their linear and nonlinear optical response, while a direct evidence of this effect has not been demonstrated up to now.

Second harmonic generation (SHG) technique is known as an extremely sensitive probe of the symmetry of nanoobjects [9, 10]. As the second order susceptibility vanishes in centrosymmetric materials, the SHG sources in case of nanostructures composed of centrosymmetric materials are localized primarily on surfaces and internal interfaces where the inversion symmetry is broken. Being a nonlinear optical probe, the SHG intensity is governed by local field distribution in a structure at the fundamental and SHG wavelengths. Resonant plasmon-assisted SHG enhancement has been observed in a variety of metallic nanostructures such as plasmonic nanocavities [11], isolated metallic nanoparticles [12], self-organized metallic nanowires [13], split-ring resonators [14], etc. It was found that pronounced SHG polarization dependencies are attained for different spatial multipoles [15,16]. Experimental observation of the SHG enhance-

#159711 - $15.00 USD Received 9 Dec 2011; revised 4 Jan 2012; accepted 5 Jan 2012; published 28 Mar 2012

ment in plasmonic nanostructures have led to new theoretical developments in this field [17,18].

New effects can be expected for the SHG in chiral nanostructures as chirality defines the symmetry of the second-order susceptibility tensor $\hat{\chi}^{(2)}$. Namely it results in the appearance of a nonzero tensor element χ_{xyz} that vanishes in achiral structures. The sign of χ_{xyz} component is determined by the handedness of the structure, which brings about the intrinsic sensitivity of the SHG response to the chirality state of a structure and allows to distinguish different enantiomers. This property has been demonstrated for *G*-shaped structures via asymmetric SHG as pronounced SHG azimuthal anisotropic dependencies were observed for the structures of different chirality, i.e. composed by *G* and mirror-*G* enantiomers [19].

In this Letter the appearance of chirality in the SHG response of planar *G*-shaped metamaterials is studied in periodic ensembles of *G*-shaped chiral nanostructures of different handedness. The differences in SHG anisotropy as well as polarization plane rotation in *G*-shaped and mirror-*G*-shaped structures prove the chiral properties of the structures under study.

2. Experimental setup and results

The samples consist of periodic arrays of *G*-shaped nanostructures made from a 25 nm thick Au film deposited onto $Si(100)/SiO_2$ substrate, the thickness of the SiO_2 layer was 200 nm. Each individual *G*-shaped structure was predefined by electron-beam lithography on an area of 1x1 μm^2. The line width and the separation between the neighbouring *G*-shaped structures is 200 nm. The experimental procedure is described in more detail in [5]. The ensembles of the so called double-periodic *G* and mirror-*G* structures were studied. Figure 1 shows the scanning electron microscopy image of one of them. Due to the composition of the samples they possess four-fold symmetry which should influence their optical response, therefore the anisotropy of optical and nonlinear-optical response of *G*-shaped structures has to be taken into consideration.

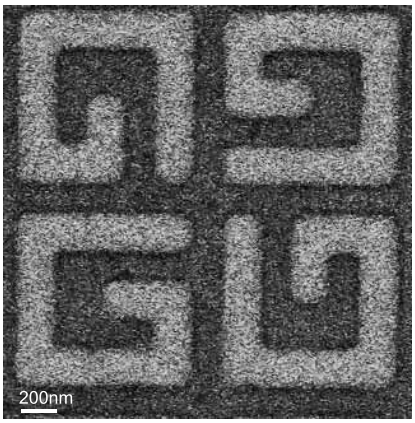

Fig. 1. SEM image of a double-periodic G-shaped structure.

For the SHG experiments the *s*-polarized radiation of a Ti:Sapphire laser was used at the wavelength of 780 nm, the pulse duration of 80 fs, the repetition frequency of 80 MHz and a mean power of 150 mW. The pump radiation was focused on the sample into a spot of 50 μm in diameter at an angle of incidence of 45°. SHG radiation reflected in the specular direction was spectrally selected by BG39 Schott color filters, passed through a diaphragm with the angular aperture of 5° and was detected by a photomultiplier operating in the photon counting mode. Pump beam polarization was controlled by $\lambda/2$ plate and the SHG polarization was detected

#159711 - $15.00 USD Received 9 Dec 2011; revised 4 Jan 2012; accepted 5 Jan 2012; published 28 Mar 2012

by Babinet–Soleil compensator and an analyzer. The appearance of chirality in the nonlinear-optical response was studied by measuring the azimuthal dependencies of the SHG radiation in the samples of different handedness, the value $\psi = 0^\circ$ corresponds to the case when the polarization plane of the fundamental beam is parallel to the side of *G*-shaped elements.

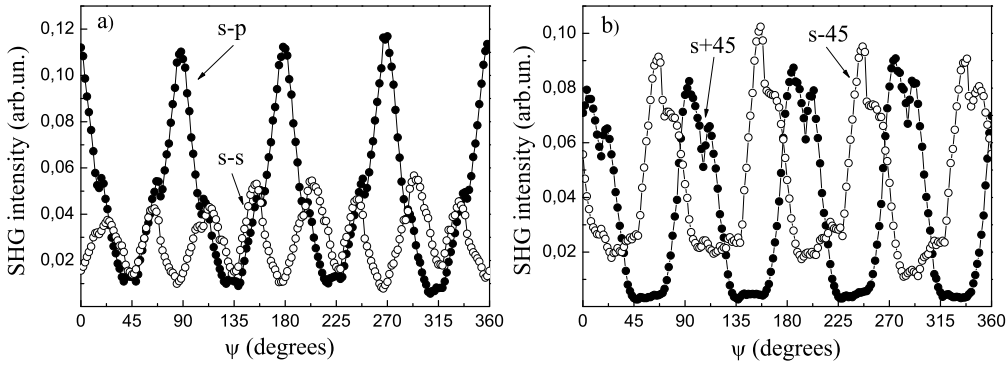

Fig. 2. Azimuthal anisotropy of the intensity of *p*, *s* (a) and *(+45°), (-45°)* (b) polarized SHG for array of *G*-shaped nanostructures under the excitation by *s*-polarized pump beam.

For the full characterization of the SHG reflected from periodic *G*-shaped structures the azimuthal dependencies of *p*, *s*, $+45^\circ$, -45° linearly polarized radiation at the double frequency along with the *right* and *left* circularly polarized SHG were studied. Figure 2 shows the SHG anisotropic azimuthal dependencies measured for one of the enantiomers for the *s*-polarized fundamental beam. Qualitatively similar dependencies were obtained for mirror-*G*-shaped structures as well, their main feature being the four-fold symmetry of the SHG pattern that shifts along the ψ axis when the SHG polarization is changed.

These measurements allowed to estimate the anisotropic dependencies of the Stokes parameters at the SHG frequency, S_0, S_1, S_2 and S_3. The S_0 parameter corresponds to the total intensity of the reflected SHG, S_1=$I_p - I_s$, S_2=$I_{+45^\circ} - I_{-45^\circ}$ and S_3=$I_{right} - I_{left}$ [20], where the superscripts *p*, *s*, $+45^\circ$, -45°, $left$ and *right* denote the corresponding polarization of the SHG radiation. The angle of the polarization plane rotation can be calculated as $\phi = -\frac{1}{2}\arctan(S_2/S_1)$ ($\phi \in [0;\pi]$). The ellipticity angle of the reflected light ε can be calculated as $\arctan(a/b)$, where *a* and *b* are the axes of the polarization ellipse. Taking into account that in the experiments we detected only coherent SHG component, the ellipticity angle was estimated using the expression $\varepsilon = \arccos(\sqrt{(\frac{S_1}{S_0})^2 + (\frac{S_2}{S_0})^2})$. Here we do not have to consider the sign of ε as it is the same for any azimuthal angle of each structure.

Figure 3 shows the anisotropy of the circularly polarized SHG intensity in double-periodic *G*-shaped metamaterials. It can be seen that four-fold azimuthal dependencies are observed for both *left*- and *right*- circular SHG polarization. The maxima of the SHG intensity are close to the azimuthal angles $\psi = 0^\circ, 90^\circ, 180^\circ, 270^\circ$ and are shifted from these values in the opposite directions for different circular polarizations. Similar features were observed for the azimuthal maxima obtained for the linearly polarized SHG (Fig. 2). Another issue to be pointed out is that the average SHG intensity is different for the *left*- and *right*- circularly polarized SHG. It is clear from Fig. 3 that the total SHG intensity averaged over all the azimuthal orientations of the samples and estimated as the square under the curve is at least twice larger for the $left$ circular SHG polarization as compared with that obtained for the *right* circular SHG polarization. The opposite situation is observed for the mirror-*G*-shaped metamaterials. In other words, we

#159711 - $15.00 USD Received 9 Dec 2011; revised 4 Jan 2012; accepted 5 Jan 2012; published 28 Mar 2012

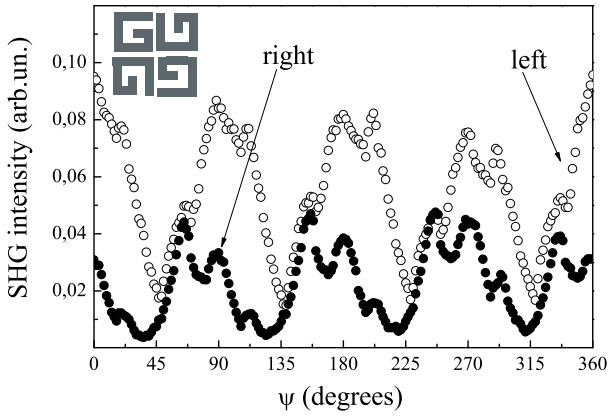

Fig. 3. Anisotropy of the the *left*- (open circles) and *right*- (filled circles) circularly polarized SHG in double-periodic array consisting of *G*-shaped nanostructures under the influence of linearly *s*-polarized fundamental radiation.

demonstrate that different efficiency for the $left-$ and $right-$ circularly polarized SHG is attained for chiral nanostructures of the opposite handedness. This is a very important conclusion that proves that we really observe different chirality of *G*- and mirror-*G* structures in the SHG response, which should not be confused with the effect of the anisotropy of the structure.

It is worth mentioning that the Stokes parameters of the fundamental radiation (780 nm) reflected from the samples were measured as well. The angle of the polarization plane rotation ϕ_ω was estimated for different azimuthal orientations of the samples. It turned out that $\phi_\omega(\psi)$ dependencies measured for the two enantiomers are very similar, the maximal value of the polarization plane rotation of about 4° was observed. No changes in the sign of $\phi_\omega(\psi)$ were detected for the two mirror *G*-structures, which means that the linear reflectivity measurements do not allow to distinguish between the two enantiomers within the experimental accuracy.

Figure 4 shows the azimuthal dependencies of the SHG polarization plane rotation $\phi_{2\omega}(\psi)$ in double-periodic *G*- and mirror-*G*-shaped structures. It can be seen from the figure that the second harmonic reflected from the samples is elliptically polarized, that is shown schematically by ellipses with the notification of the handedness of the rotation. Moreover, we observe that the orientation of the main axis of the SHG polarization ellipse corresponds to the *p*-polarization at $\psi = 0$, then it changes continuously to *s*-polarization for $\psi = 40^\circ$ and then back to *p*-polarization ($\psi = 90^\circ$). This scenario is periodic in $\pi/2$. In other words, linearly *p*-polarized SHG is observed as the polarization plane of the pump beam is parallel to the sides of *G*-elements, i.e. for the azimuthal angles $\psi = n \cdot \pi/2, n = 0,1,2...$, while it is *s*-polarized as the polarization plane of the fundamental beam is parallel to the diagonals of the sample. The corresponding azimuthal angles are 40°, 130°, 220° and 310° and we can consider them as those corresponding to the maximal SHG polarization plane rotation.

It is worth noting that $\phi_{2\omega}(\psi)$ dependencies are also four-fold symmetric and look like mirror images for *G*- and mirror-*G* structures. It means that the direction of the SHG polarization plane rotation is opposite for the two enantiomers in accordance with the different handedness of these structures. In other words, we have shown that the effects of the SHG polarization plane rotation can be exploited for distinguishing between the enantiomers of planar chiral nanostructures.

#159711 - $15.00 USD Received 9 Dec 2011; revised 4 Jan 2012; accepted 5 Jan 2012; published 28 Mar 2012

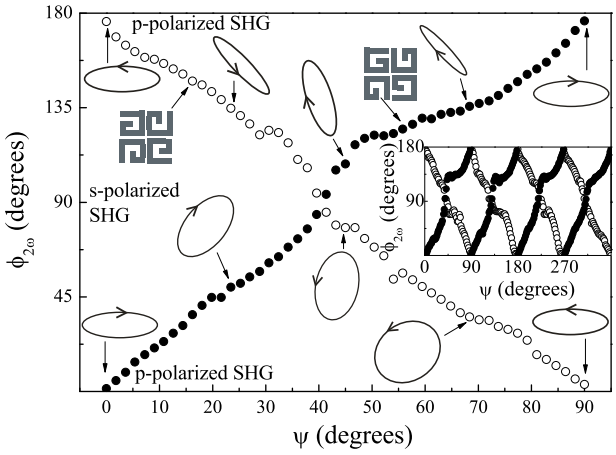

Fig. 4. Azimuthal dependence of the SHG polarization plane rotation for the double-periodic arrays of *G*-shaped (filled circles) and mirror-*G*-shaped (open circles) nanostructures. The angle of SHG polarization plane 0° and 180° corresponds to the *p*-polarized SHG and 90° - *s*-polarized SHG. For the azimuthal angles 0°, 22.5°, 90°, 67.5° and 90° polarization states are shown for both samples.

3. Discussion

When discussing the possible mechanisms of the observed dependencies we should first of all refer to the previous studies [5, 21] where a strong anisotropy of the linearly polarized SHG was observed for similar structures. It was proved that the main effect to play a role in this anisotropy is the different local field distribution at the fundamental wavelength for different azimuthal orientation of the samples. This stems from the expression for the SHG intensity [21]: $I_{2\omega} \propto \left\langle (\hat{\chi}^{(2)} L_{2\omega}(\psi) L_{\omega}^2(\psi))^2 \right\rangle I_{\omega}^2$, where $L_{\omega}, L_{2\omega}$ are the local field factors at the fundamental and SHG wavelengths, I_{ω} is the pump intensity and the brackets denote the statistical averaging over the laser spot area.

We suppose that in our case different anisotropy of the fundamental field local factor is achieved for the two mirror *G*-shaped structures, which results in antisymmetric azimuthal dependencies of the polarization plane rotation for the two enantiomers. Thus different handedness of the structures results in antisymmetric distribution of the local fields of different polarizations, that governs the direction of the SHG polarization plane rotation.

At the same time, no such effects are observed for the case of linear-optical response from the same structures. This is possible due to an intrinsically much less structural and field sensitivity of the linear response.

4. Conclusions

In conclusion, the anisotropy of the circularly polarized SHG in planar arrays of two-period gold *G*-shaped nanostructures is studied. A significant rotation of the polarization plane of the reflected SHG is detected. The polarization plane rotation of up to 90° is attained as the polarization plane of the fundamental beam is oriented along the diagonal to the *G*-element. The azimuthal dependencies of the polarization plane rotation of the fundamental beam are similar for the two enantiomers, while they are found to be of the opposite signs in case of the SHG. It should be stressed that these results are valid under the used experimental conditions, i.e. at the pump wavelength of 780 nm and the angle of incidence of 45 degrees.

#159711 - $15.00 USD Received 9 Dec 2011; revised 4 Jan 2012; accepted 5 Jan 2012; published 28 Mar 2012